JOURNAL OF PROPULSION AND POWER
Vol. 17, No. 6, November–December 2001

Significance of Fuel Selection for Hypersonic Vehicle Range

Mark J. Lewis*
University of Maryland, College Park, Maryland 20742-3015

Optimization studies of engine-integrated hypersonic aircraft for both cruising and accelerating missions tend to demonstrate noticeably lower lift-to-drag ratios than those of pure aerodynamic forms. One explanation of this is that, with low-density fuels such as hydrogen, matching lift to weight results in configurations that cannot take advantage of high-lift aerodynamics, especially when they operate at high dynamic pressures for airbreathing propulsion. Hydrogen has been the fuel of choice for hypersonic flight because of its rapid burning rate, high specific energy content, and good heat transfer properties for active cooling and recuperation. In contrast, hydrocarbon fuels have much longer burn times and substantially lower specific energies, although they have substantial packaging and handling advantages. To study this, range performance is evaluated in terms of fuel density for hypersonic craft with time-varying lift-over-drag ratio. Historical data and geometric scaling are used to show that with hydrocarbon fuels, which have an order of magnitude greater density than hydrogen, hypersonic cruiser designs can take greater advantage of optimal aerodynamics. As such, hydrocarbon engine-integrated vehicles may have comparable or superior cruise range performance in comparison to cryogenically fueled designs.

Nomenclature

A_{ref}	=	force coefficient reference area
a	=	zero-lift-drag constant
b	=	scaled drag due to lift
$C_{D,0}$	=	zero-lift drag
c_1, c_2, c_3	=	vehicle scaling constants
D	=	drag
g	=	gravitational acceleration, 9.81 m/s^2
$\bar{g}$	=	centrifugal acceleration, normalized to gravity
h	=	fuel heating value, MJ/kg
I_{sp}	=	specific impulse
k	=	drag due to lift proportionality
L	=	lift
M	=	Mach number
m	=	tank weight powerlaw coefficient
n	=	drag due to lift powerlaw coefficient
q_∞	=	freestream dynamic pressure
R	=	range
T	=	thrust
u_0	=	cruise flight velocity
V	=	volume
W	=	weight, kg · f
ε	=	fuel weight fraction
η	=	efficiency
λ	=	payload weight fraction
ρ_f	=	fuel density
ρ_∞	=	freestream air density
Ω	=	normalized lift coefficient

Subscripts

c	=	cruise value
D	=	drag
L	=	lift
∞	=	freestream

Introduction

HYDROCARBON fuels possess many operational advantages for application to hypersonic flight when compared to hydrogen. With the exception of cryogenic methane, hydrocarbons are storable, and their handling is familiar. In contrast, a hydrogen-fueled craft would have to be loaded just before launch, and its tanks would have to be designed to handle the extra thermal stresses associated with storing cryogenic fuel inside a vessel with an outside heated by hypersonic aerothermodynamics.

Despite handling and safety issues, hydrogen has often been cited as the airbreathing fuel of choice at hypersonic Mach numbers because of its rapid burning and high mass-specific energy content. Indeed, for the airbreathing transatmospheric flight envelope, hydrogen is the only likely fuel that might deliver net positive thrust up to near-orbital velocities. For a cruiser operating below Mach 10, or the first stage of a two-stage-to-orbit system, these combustion advantages may be of less importance, and the packaging and handling benefits of hydrocarbon fuels may result in superior overall performance.

Hydrogen has very low density, and it has boil-off problems, leading to packaging challenges that drive up structural mass and required overall volume for a given mission. Cryogenics such as hydrogen and methane will also have obvious handling problems. In contrast, hydrocarbons are slower burning and have between two-fifths and one-third the energy per unit mass compared to hydrogen; however, with up to 11 times the storage density, they have over $3\frac{1}{2}$ times more energy content per unit volume.[1] The properties of various hydrocarbons are summarized in Table 1, contrasted with cryogenic hydrogen in both liquid and slush form.[2–5] Note that hydrocarbons contain approximately 15–20% hydrogen, and so they actually store hydrogen at up to twice the density of pure cryogenic hydrogen.

Conventional hydrocarbon fuels can be divided into two basic categories: methane, with energy density of 50 MJ/kg and specific gravity of about 0.4 (and also cryogenic storage requirements), and the JP hydrocarbons, with nearly twice the density but only 40 MJ/kg specific energy content. Interestingly, even endothermic fuels such as methylcyclohexane (MCH) have about the same storage properties and combustion energy content as the JP fuels, though they may have advantages in recuperating combustion heat. Hydrogen as either liquid or slush has about the same energy content, with a slight difference due to the heat of fusion, but slush has about a 15% higher density than the liquid form.

Overall, this means that, from a packaging standpoint, a hydrocarbon-fueled vehicle will be much more dense than a comparable hydrogen craft, giving it greater lift-load requirements (i.e., smaller planform area for a given L/D ratio), which correspond to a greater volumetric efficiency. The question to be explored in this paper is whether the advantages of higher energy per unit mass in

Received 13 August 2000; revision received 20 November 2000; accepted for publication 29 December 2000.

*Professor, Department of Aerospace Engineering. Associate Fellow AIAA.

Table 1 Energy properties of H_2 and hydrocarbon fuels data complied from Refs. 2–5

Fuel	Energy/Mass, MJ/kg	Energy/Volume, MJ/l	STP density, kg/m^3
Liquid H_2	116.7	8.2	71
Slush H_2	116.6	9.8	82
Methane	50.0	20.8	424
n-Heptane	44.6	30.3	717
JP-4	43.5	33.1	760
JP-5	43.0	35.1	815
JP-7	43.9	34.7	790
JP-8	43.2	35.0	809
Jet A	43.4	34.6	799
Kerosene	42.8	34.2	800
MCH	43.4	33.4	770

hydrogen outweigh the packaging advantages of higher energy per unit volume for hydrocarbon, especially for a cruiser whose performance will be measured primarily by distance traveled for a given total weight.

Hydrogen has also been cited as the most practical fuel for active cooling on leading-edge surfaces and engine components. However, the endothermic hydrocarbon fuels such as MCH have also received some attention as a viable means for channeling surface heat back into useful propulsion energy. There are several unknowns about these fuels, such as those related to the combustion rates and health hazards of the endothermic fuel products (in the case of MCH, slow-burning, potentially carcinogenic toluene is produced), as well as the overall cost and required infrastructure to support the use of such exotics. A related and particularly promising technology would be the steam reforming of hydrocarbons through chemical regeneration, relying on the endothermic steam reforming process to cool leading-edge surfaces and possibly engine parts and to produce methane and hydrogen for combustion.[6] This process may be thought of as taking advantage of hydrocarbons actually storing hydrogen at higher density than pure cryogenic hydrogen, as cited earlier. It is clear from the values presented in Table 1 that, if viable for cooling, endothermics can be used with about the same packaging properties as other hydrocarbons.

Cruiser Range vs Fuel

Because hydrocarbon appears to be a viable fuel for the moderate (and most immediately realistic) hypersonic range of flight Mach number less than 10, and because it is more easily handled and storable, there is great value in studying the impact of such fuels in optimal vehicle configurations. One indication is the effect of fuel choice on range. It can be shown that the higher lift coefficient requirements of a hydrocarbon-fueledcraft are actually an advantage in the hypersonic Mach number range because practical configurations for these vehicles tend to operate in a regime where L/D increases with increasing lift coefficient.[7,8]

If the time rate of change in total energy (potential plus kinetic) is equal to the net thrust power (thrust minus drag times velocity) and lift equals weight, the so-called total energy formulation[9] can be arranged to show that

$$\mathrm{d}R = -u_0 I_{\mathrm{sp}} \left[\frac{L}{D}\right] \frac{\mathrm{d}W}{W} - \left[\frac{L}{D}\right] \mathrm{d}\left(h + \frac{u_0^2}{2g}\right) \tag{1}$$

For low-speed vehicles, a simple approximation is to take L/D, velocity, and specific energy as constant, resulting in one form of the well-known Breguet range equation: $R = u_0 I_{\mathrm{sp}}[L/D]\ \ell n\{W_{\mathrm{init}}/W_{\mathrm{final}}\}$. A hypersonic craft will be traveling at sufficient speed for centrifugal effects to be important. The effective weight of a hypersonic craft will be $W' = W(1 - u_0^2/rg)$, so that range at constant velocity and constant L/D is

$$R = \frac{u_0 I_{\mathrm{sp}}}{(1-\bar{g})} \left[\frac{L}{D}\right] \ell n \frac{W_{\mathrm{initial}}}{W_{\mathrm{final}}} \tag{2}$$

where $\bar{g} = u_0^2/rg$, the ratio of centrifugal to gravitational acceleration. When an overall fuel weight fraction, $\varepsilon \equiv W_{\mathrm{total\ fuel}}/W_{\mathrm{gross\ takeoff}}$ and the cruise portion of the fuel weight fraction $\varepsilon_c \equiv W_{\mathrm{cruise\ fuel}}/W_{\mathrm{gross\ takeoff}}$ are defined,

$$\begin{aligned} R &= \frac{u_0 I_{\mathrm{sp}}}{(1-\bar{g})} \left[\frac{L}{D}\right] \ell n \left\{\frac{1}{1-\varepsilon_c}\right\} \\ &\cong \frac{u_0 I_{\mathrm{sp}}}{(1-\bar{g})} \left[\frac{L}{D}\right] \left\{\frac{2.8257\varepsilon_c^3 - 7.9490\left(\varepsilon_c^2 - \varepsilon_c\right)}{(2-\varepsilon_c)^3}\right\} \end{aligned} \tag{3}$$

where the second line is written with an algebraic approximation to the natural logarithm function, which has $\mathcal{O}(10^{-3})$ accuracy for values of $\varepsilon < 0.7$. The cruise fuel weight fraction will obviously be smaller than the total fuel weight fraction because some fuel must also be used for takeoff and acceleration, deceleration, and landing, as well as reserve. Historically, the fuel used to cruise is approximately 89% of the total supply, but this could be smaller for a hypersonic vehicle with relatively long acceleration and deceleration phases.[9]

It is possible for the second term on the right-hand side of Eq. (1) to be significant for a hypersonic aircraft. At hypersonic speeds, kinetic energy will generally exceed the potential energy, and, thus, the specific energy might be changed during the cruise. Even with constant total specific energy, it can be shown that periodic trajectories that trade kinetic energy with potential energy have range advantages over constant altitude, constant velocity trajectories.[10] Optimal periodic trajectories that cycle the engine, producing thrust at the high dynamic pressures at minimum altitude, have been shown to be especially advantageous in extending aircraft range over that of level cruise flight. These periodic trajectories do require engine cycling and may yield unpleasant accelerations that might limit their application to inhabited hypersonic vehicles. Regardless of being level or periodic, optimal range trajectories tend to seek constant specific energy. Under such conditions, if the hypersonic airbreathing engine requires constant dynamic pressure and is powered continuously through the flight, the vehicle will be constrained to fly at nearly constant velocity and constant altitude.[11] These assumptions will be carried through the following analysis.

For many craft, including a hypersonic vehicle, constant L/D is a poor assumption because of the large variation in overall weight during a cruise flight. To match decreasing weight, lift must be reduced, and, thus, L/D may change. This decrease in lift might be realized by flying to lower dynamic pressure, flap adjustments, or change in vehicle attitude; the last is most likely because reduced dynamic pressure may inhibit successful combustion in a hypersonic airbreathing engine, and substantial flap deflections will generally increase drag significantly. Thus, constant velocity is also a reasonable hypersonic cruise assumption as is constant dynamic pressure.

When drag is decomposed into an angle-independentcomponent (including skin-friction, leading-edge, and base effects) and wave drag, which can be written as drag due to lift with $C_{D,\mathrm{lift}} = kC_L^n$,

$$L/D = C_L \Big/ \left(C_{D,0} + kC_L^n\right) \tag{4}$$

which is plotted in Fig. 1 for two representative values of minimum drag coefficient and $k = 1$. The constant k and the zero-lift drag determine the maximum achievable L/D because

$$\begin{aligned} \left[\frac{L}{D}\right]_{\max} &= \frac{1}{nk^{1/n}} \left[\frac{n-1}{C_{D,0}}\right]^{1-1/n} \\ &= \frac{1}{3}\left[\frac{4}{k^2 C_{D,0}}\right]^{\frac{1}{3}} \qquad n = 1.5 \\ &= \frac{1}{2\sqrt{kC_{D,0}}} \qquad n = 2 \end{aligned} \tag{5}$$

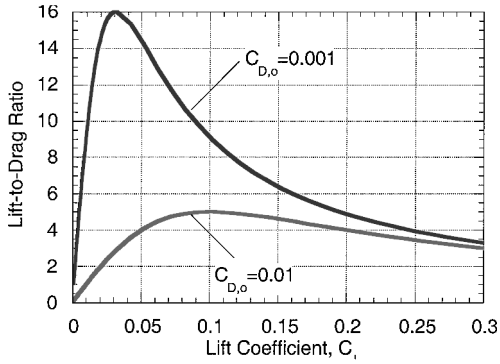

Fig. 1 L/D vs C_L for $k = 1$ and $C_{D,0} = 0.001$ and 0.01.

At maximum L/D, $C_{D,0} = (n-1)kC_L^n$, meaning that optimal designs generally have from one-half to two-thirds of the drag in wave drag, depending on n. The prediction of hypersonic tangent wedge theory is $n = 2$, $k = 3/(8[\gamma+1]\theta)$, where θ is the surface angle of obliquity; in the linear-theory limit, $k = M/4$, and, therefore, depends on Mach number, and in the Newtonian limit, $n = 1.5$ and $k = 1$, independent of Mach number.[12] For the vehicles of interest here, typical aerodynamic configurations will have values of $1.5 < n < 2$ and $k \sim 1$–1.5, consistent with experimental measurements.[13]

The L/D ratio can be written in terms of maximum available L/D performance:

$$\frac{L}{D} = \frac{4kC_L}{[L/D]_{\max}^{-2} + 4k^2C_L^2} \tag{6}$$

The maximum L/D occurs at a lift coefficient $C_{L,\max L/D} = \sqrt{(C_{D,0}/k)}$. This value of C_L is generally different from the maximum possible C_L, which will typically coincide with small values of L/D. This maximum value thus represents an aerodynamic performance that may not be achieved in a practical integrated cruise vehicle with lift matched to weight. This is because the required value of lift coefficient, as set by the total weight, planform area, and engine-determined dynamic pressure, may dictate a value of L/D that is less than can be achieved without the matching constraints.

If lift coefficient is below the value for maximum L/D, it will be beneficial to L/D to increase the effective loading, that is, increase average vehicle density at a given dynamic pressure. Conversely, if C_L is above the value for maximum L/D, decreasing the effective loading will increase achieved L/D. Note that this analysis does not explicitly include contributions to lift from the engine, which may be hard to separate from aerodynamic lift on a hypersonic craft. Also note that trim adjustments as the vehicle lift is reduced may have the effect of reducing drag, thereby reducing the sensitivity of L/D to C_L; this effect is equivalent to reducing the value of k in Eq. (4) by some vehicle-specific factor.

When Eq. (1) is integrated with the changing L/D of Eq. (4), the range is

$$R = u_0 I_{\text{sp}} \int_{W_{\text{init}}}^{W_{\text{final}}} \frac{\mathrm{d}W}{a + b(1-\bar{g})W^n} \tag{7}$$

with constants $a = q_\infty A_{\text{ref}} C_{D,0}$ and $b = k(q_\infty A_{\text{ref}})^{1-n}$, where dynamic pressure is $q_\infty = \frac{1}{2}\rho u_0^2$. With integration of $n = 2$, a reasonable assumption for slender hypersonic shapes, the range equation follows an inverse tangent function, not the logarithmic function for constant L/D:

$$R = \frac{u_0 I_{\text{sp}}}{(1-\bar{g})\sqrt{kC_{D,0}}} \left\{ \tan^{-1}\left(\frac{W_{\text{init}}(1-\bar{g})}{q_\infty A_{\text{ref}}} \sqrt{\frac{k}{C_{D,0}}} \right) - \tan^{-1}\left(\frac{W_{\text{final}}(1-\bar{g})}{q_\infty A_{\text{ref}}} \sqrt{\frac{k}{C_{D,0}}} \right) \right\} \tag{8}$$

Equation (8) is equivalent to the range expression first derived by Bert for jet aircraft with varying L/D flying at constant altitude.[14] To solve the range equation in terms of fuel density and specific energy, it is useful to write the weight ratio terms as a function of the fuel weight fraction ε_c and a normalized lift load defined as:

$$\Omega \equiv \frac{W_{\text{init}}(1-\bar{g})}{q_\infty A_{\text{ref}}} \sqrt{\frac{k}{C_{D,0}}} = 2kC_{L,\text{init}} \left[\frac{L}{D}\right]_{\max} = \frac{C_{L,\text{init}}}{C_{L,\max L/D}} \tag{9}$$

The range is then

$$R = \frac{2u_0 I_{\text{sp}}}{(1-\bar{g})} \left[\frac{L}{D}\right]_{\max} \tan^{-1}\left\{ \frac{\varepsilon_c \Omega}{[1-\varepsilon_c]\Omega^2 + 1} \right\}$$

$$\cong \frac{2u_0 I_{\text{sp}}}{(1-\bar{g})} \left[\frac{L}{D}\right]_{\max} \left\{ \frac{[1-\varepsilon_c]\varepsilon_c\Omega^3 + \varepsilon_c\Omega}{[1-\varepsilon_c]^2\Omega^4 + 2\left[1-\varepsilon_c+0.14\varepsilon_c^2\right]\Omega^2 + 1} \right\} \tag{10}$$

In the second line of Eq. (10), an approximation for the inverse tangent function has been used to write the range in an algebraic form. The algebraic form of Eq. (10) permits ready exploration of design limits. Note that this range equation now has two mass-fraction variables: ε_c and Ω, both of which are dependent on the average density of the vehicle.

For representative weight fraction values of $\varepsilon_c = 0.5$ and 0.7,

$$R|_{\varepsilon=0.5} = \frac{\eta h}{g(1-\bar{g})} \left[\frac{L}{D}\right]_{\max} \left\{ \frac{0.50\Omega^3 + \Omega}{0.25\Omega^4 + 1.07\Omega^2 + 1} \right\}$$

$$R|_{\varepsilon=0.7} = \frac{\eta h}{g(1-\bar{g})} \left[\frac{L}{D}\right]_{\max} \left\{ \frac{0.42\Omega^3 + 1.40\Omega}{0.09\Omega^4 + 0.7372\Omega^2 + 1} \right\} \tag{11}$$

These are plotted in Fig. 2, normalized to thrust power.

It is interesting to probe the extremes of Eq. (10). In the limit of very large Ω, which represents a very high average density craft,

$$R \approx \frac{2\eta h}{g(1-\bar{g})} \left[\frac{L}{D}\right]_{\max} \left(\frac{\varepsilon_c}{1-\varepsilon_c}\right) \frac{1}{\Omega} \tag{12}$$

Conversely, in the limit of very large reference area to weight, that is, very small Ω, corresponding to a very low density craft, range is directly proportional to weight per reference area:

$$R \approx \frac{2\eta h}{g(1-\bar{g})} \left[\frac{L}{D}\right]_{\max} \varepsilon_c \Omega \tag{13}$$

Higher-density fuel can, therefore, offer either a range advantage or disadvantage, depending on the relative size of the craft. Most vehicles of interest will have values of Ω between about 0.5 and 5 and values of ε between 0.5 and 0.9, and so actual craft will not

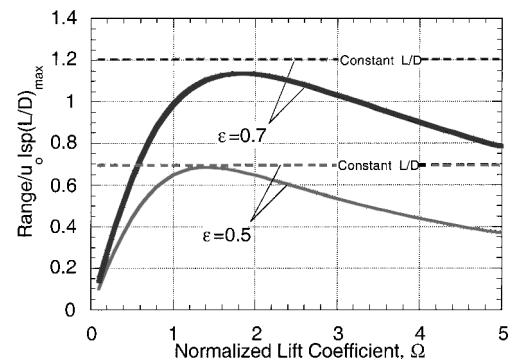

Fig. 2 Range, normalized to flight velocity times I_{sp} times maximum aerodynamic L/D, for fuel weight fractions $\varepsilon = 0.5$ and 0.7, as a function of normalized lift coefficient Ω; also shown are normalized ranges if L/D is constant during entire flight.

approach these limits of Eqs. (12) and (13). However, these results suggests that there is, for any mission and vehicle class, an optimum average vehicle density, which may be arrived at by a combination of several fuels.

More generally, neglecting the distinction between overall ε and ε_c, the sensitivity of range to the choice of L/D, ε, and Ω is as follows:

$$\frac{\partial R/R}{\partial[L/D]/[L/D]} = 1 \tag{14}$$

$$\frac{\partial R/R}{\partial \varepsilon/\varepsilon} \approx \frac{[1-\varepsilon]^2\Omega^4 + 2[1-\varepsilon+0.14\varepsilon^2]\Omega^2 + 1}{-[\varepsilon-1]^3\Omega^4 + [\varepsilon^2 - 3\varepsilon + 2]\Omega^2 + 1} \tag{15}$$

$$\frac{\partial R/R}{\partial \Omega/\Omega} \approx \left(\frac{1-[1-\varepsilon]\Omega^2}{1+[1-\varepsilon]\Omega^2}\right) \times \frac{[1-\varepsilon]^2\Omega^4 + 2[1-\varepsilon+0.14\varepsilon^2]\Omega^2 + 1}{[\varepsilon-1]^2\Omega^4 + [\varepsilon^2 - 2\varepsilon + 2]\Omega^2 + 1} \tag{16}$$

The range sensitivities with respect to ε and Ω are plotted in Fig. 3 for representative values of ε, as a function of Ω. Note that for these typical values, when L/D is varying through the flight according to the assumptions of Eq. (4), range is more sensitive to fuel weight fraction than maximum L/D and least sensitive to initial lift coefficient. This once again indicates the importance of packaging efficiency and, therefore, increased fuel density, in determining range. The derivative of range with respect to fuel weight fraction is always positive, meaning that the range always increases when fuel weight fraction increases.

Note that the derivative with respect to normalized lift coefficient Ω has a zero value for each fuel weight fraction ε. For smaller values of Ω, the derivative is positive, but for large values it is negative. The zero point corresponds to a vehicle that has an optimum value of lift coefficient, traversing the L/D peak in Fig. 1. For very small values of Ω, the vehicle is flying on the far left side of Fig. 1, at a low L/D; for very large values of Ω, the vehicle is on the far right side of Fig. 1, also at low L/D. Note that the estimated value for a hydrocarbon hypersonic craft is in the range of $\Omega \sim 2$–4, very close to this optimal zero point in the derivative of range with respect to Ω. Hydrogen-fueled craft, with $\Omega \sim 0.4$–0.7, are operating in a regime in which increase in lift coefficient (i.e., increasing vehicle density or decreasing dynamic pressure) will increase range.

Specific Impulse and Fuel Selection

Accounting for the effect of fuel selection on $u_0 I_{sp}$ in the range equation requires an estimate for the scaling of thrust power with fuel specific energy. Specific impulse times flight velocity is the thrust power divided by weight flow rate of fuel, so that $u_0 I_{sp} = \eta h/g$, which is overall efficiency η times the fuel heating value h (reported as energy per unit mass of fuel consumed) divided by gravitational acceleration g (Ref. 15). This leads to the result that the product of velocity times specific impulse should be roughly constant for a given fuel type (and of course engine class). A hydrogen-fueled scramjet, with specific energy of 119.6 MJ/kg, should, therefore, have 2.85 times the thrust power of a comparable hydrocarbon-fueled engine. The analysis of Ref. 16 predicts that hydrogen scramjets will have $I_{sp} = 3000$ s at Mach 6, $I_{sp} = 2500$ s at Mach 8, $I_{sp} = 2000$ s at Mach 10, and $I_{sp} = 1200$ s at Mach 15. These all correspond to overall thrust-power efficiencies of ~50%. Corresponding hydrocarbon scramjet performance will be $I_{sp} = 1000$ s at Mach 6, $I_{sp} = 880$ s at Mach 8, and $I_{sp} = 700$ s at Mach 10, the last assuming it is even possible to operate a hydrocarbon scramjet above Mach 8 (Ref. 6). With endothermic fuels and reformation techniques, hydrocarbon specific impulse might be increased significantly.

Overall efficiency η includes propulsive and thermodynamic losses. This means that the first two terms in the range equation should scale approximately in proportion to fuel energy per unit mass, assuming constant efficiency. The efficiency η may, in fact, be very different for hydrocarbon and hydrogen fuels, especially given differences in mixing, combustion rates, and recuperative properties, though consideration of such is beyond the scope of this treatment.

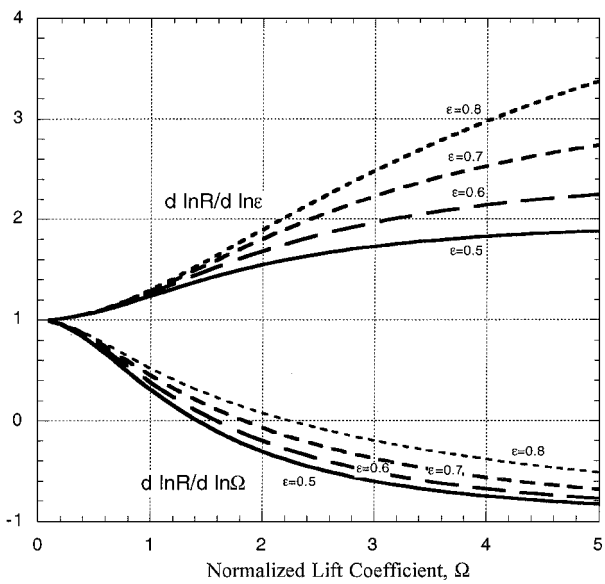

Fig. 3 Logarithmic derivative of range with respect to fuel weight fraction ε and normalized lift coefficient Ω.

Baseline Vehicle Model

Because range depends on both ε and Ω, it is of interest to compare likely values for these parameters for both hydrogen and hydrocarbon craft. To estimate practical values for Ω, it is most useful to compare within shapes with the same basic geometry. Once a baseline value of normalized weight Ω is estimated, values can be scaled for different vehicle densities. For a given class of geometries, the aerodynamic force coefficient reference area will scale with volume as $a_{ref} = c_3 V^{2/3}$, where c_3 is a volumetric efficiency, so that fixed total weight Ω, which is inversely proportional to reference area, is directly proportional to $(\rho_f)^{2/3}$.

There is no historical database for hydrogen-fueled craft for sizing estimates. An optimized hydrogen-fueled cruiser has been designed and described in Ref. 17 and will be used to scale a hydrogen-fueled baseline. This vehicle is a Mach 10 cruiser operating at dynamic pressures of about 1 atm, with airframe $L/D = 3.78$ and 864 m^2 planform area (shown in Fig. 4), and is very similar to the dual-fuel vehicle described in Ref. 18, except that it employs waverider aerodynamics for optimum L/D. The vehicles of Refs. 17 and 18 use both hydrocarbon and hydrogen fuel, with approximately 90% hydrogen and 10% JP-7, by volume. The JP-7 powers lower-speed engines, which can be refueled in air. The 7300 km range craft of Ref. 17 has a fuel weight fraction of $\varepsilon = 0.58$ and $\Omega = 0.33$ with total mass of 226,600 kg. Lift coefficient of this range-optimized vehicle is $C_L = 0.0313$, and $C_D = 0.00829$ at 48 kPa dynamic pressure, required for efficient scramjet combustion. The hydrogen-fueled hypersonic vehicles described in Refs. 7 and 8 also had $\varepsilon = 0.58$, with average density of 124 kg/m^3.

Note that the baseline configuration of Fig. 4 is a single-point design that has been optimized with lift constrained to equal weight, resulting in a value of L/D, which is less than half the maximum value for a pure waverider airframe, as explained earlier. That does not imply that this specific vehicle could be flown with much higher L/D; instead, the configuration in Fig. 4 belongs to a family of shapes that could be optimized to provide higher L/D if dynamic pressure were not constrained by the engine requirements.

Figure 5 presents the relative range performance of JP- and methane-fueled craft, compared to a hydrogen-fueled vehicle. A hydrocarbon craft operating at Mach 8 with the same total weight and fuel fraction would have $\Omega = 2.94$ which translates into ~60% of the range of the hydrogen-fueled craft with the same total initial weight and fuel fraction. The fuel weight fraction of the hydrocarbon-fueled craft should be somewhat higher than the baseline hydrogen design.

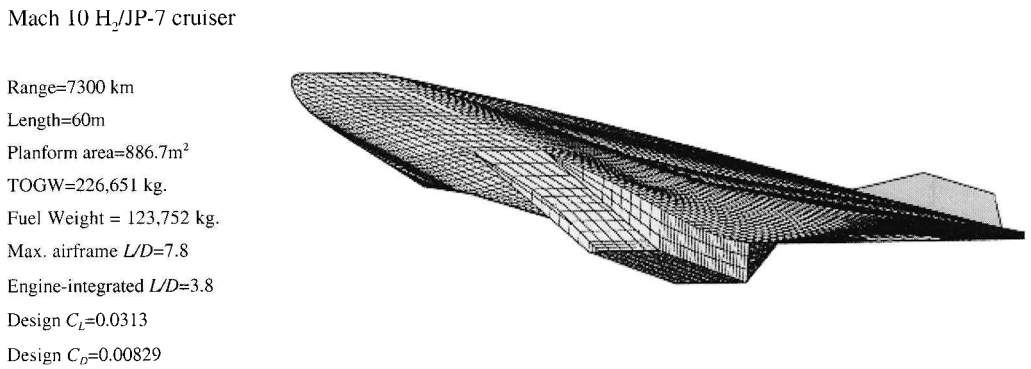

Fig. 4 Baseline hypersonic reference vehicle, used for scaling range performance.

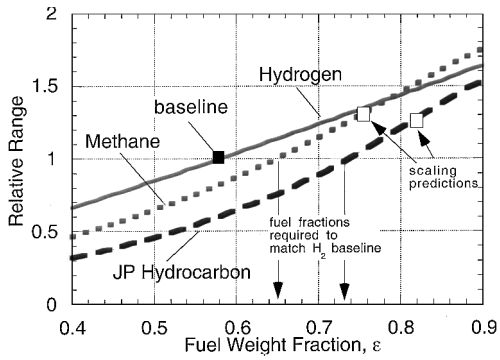

Fig. 5 Relative range of Mach 10 hydrogen and Mach 8 hydrocarbon-fueled craft, as a function of fuel weight ratio, compared to a baseline 15-km range craft.

Higher-density hydrocarbon fuels will have smaller tanks compared to low-density (and, thus, high volume) hydrogen fuel, which will in turn increase the relative ε of the hydrocarbon design. There is, unfortunately, no known detailed study for a hydrocarbon-only hypersonic cruiser comparable to the vehicles presented in Refs. 17 and 18, and so the hydrocarbon vehicle must be sized with appropriate scaling assumptions. Raymer[9] has fit historical data for a wide range of aircraft types and weights and has provided powerlaw curve fits for the empty weight fraction as a function of total weight. The general trend is that the empty weight fraction decreases as total weight increases, which is equivalent to fuel weight fraction increasing with total weight.[9] This is not surprising, given the increased volumetric efficiency of a larger aircraft. Though there is obviously no historical database for hypersonic cruisers, they might be compared to long-range bombers, with an empirically correlated behavior of $\varepsilon \approx 1 - 1.033 W_T^{-0.7}$ where W_T is the weight measured in newtons. For a 100,000-kg aircraft, this yields $\varepsilon = 0.61$; at 1,000,000 kg, $\varepsilon = 0.67$. For comparison, the fuel fraction of the JP-7-powered SR-71, with total mass of 75,600 kg, is estimated at $\varepsilon = 0.62$; for the 899,500-kg Concorde, $\varepsilon = 0.67$, and for the 242,540-kg delta-wing XB-70, powered by JP-6, $\varepsilon = 0.63$.

The volumetric efficiency, defined as the ratio of (volume)$^{2/3}$ over surface area, of the historical vehicles cited is generally lower than for blended lifting body shapes envisioned for hypersonic flight. For instance, the volumetric efficiency of the XB-70 is approximately 2%, compared to 10–20% efficiencies for blended hypersonic forms.[19] Given that fuel weight fraction will increase with increasing volumetric efficiency, it is not unreasonable to assume that a packaging-optimized hypersonic hydrocarbon craft could have $\varepsilon = 0.7$ or higher. As shown in Fig. 5, with $\varepsilon = 0.7$, the hydrocarbon craft would have 90% of the range of the hydrogen vehicle. At $\varepsilon = 0.8$, which is clearly an optimistic value, the hydrocarbon craft has 25% greater range than hydrogen craft with a 58% fuel weight fraction.

Fuel Fraction vs Fuel Density

To scale fuel weight fraction in more detail, tank weight is modeled as a function of the volume of contained fuel, such that $W_{\text{tank}} = c_1 V_{\text{fuel}}^m$ where m should be between one-half, for a cylindrical tank with fixed wall thickness, and one, for a spherical tank with constant pressure. The tank in this case includes the integral fuel-containing structure and associated mass and subsystems. Note that historical correlations of rocket tank mass in Ref. 20 generally indicate that cryogenic hydrogen tank mass scales linearly with contained fuel mass, whereas hydrocarbon fuel tanks scale with the 0.6 power of fuel mass.[20] These correlations were actually derived from both high-speed aircraft and rockets, and it can therefore be argued that a hypersonic aircraft hydrocarbon tank will scale with approximately the one-half power of fuel mass, whereas the hydrogen tank mass will scale in proportion to fuel mass. The added weight from the thermal protection system, also a function of surface area, will obviously complicate this scaling.

It is assumed that the total vehicle volume is proportional to the fuel volume.[17] When engine weight is modeled as proportional to maximum thrust, and payload as proportional to total weight, $W_{\text{engine}} + W_{\text{payload}} = c_2 W_{\text{initial}}$, with

$$c_2 = \frac{\lambda + 1}{[L/D]_{\max}[T/W]_{\text{engine}}} \tag{17}$$

where λ is the payload weight fraction. Fuel weight fraction can be written for a given initial weight in terms of fuel density ρ_f:

$$\varepsilon = \frac{[1-c_2]W_{\text{fuel}}}{W_{\text{fuel}} + W_{\text{tank}}} = \frac{[1-c_2]\rho_f g V_{\text{fuel}}}{\rho_f g V_{\text{fuel}} + c_1 V_{\text{fuel}}^m}$$

$$= \frac{[1-c_2]\rho_f g)^m}{(\rho_f g)^m + c_1(\varepsilon W_{\text{initial}})^{m-1}} \tag{18}$$

For the fuel weight fraction,

$$\varepsilon^m + \left[\frac{(\rho_f g)^m}{c_1 W_{\text{initial}}^{m-1}}\right]\varepsilon - \left[\frac{(1-c_2)(\rho_f g)^m}{c_1 W_{\text{initial}}^{m-1}}\right] = 0 \tag{19}$$

which has two important closed-form solutions:

$$\varepsilon|_{m=1} = \frac{(1-c_2)\rho_f g}{\rho_f g + c_1}$$

$$\varepsilon|_{m=\frac{1}{2}} = 1 + \frac{c_1^2}{2\rho_f g W_{\text{initial}}} - c_2$$

$$- \frac{c_1}{\sqrt{\rho_f g W_{\text{initial}}}}\sqrt{1 + \frac{c_1^2}{4\rho_f g W_{\text{initial}}} - c_2} \tag{20}$$

If tank/structural weight is scaled linearly with volume, that is, $m = 1$, the constant of proportionality for hydrogen fuel is $c_1 = 490$ N/m^3 for the baseline vehicle. If tank weight is calculated for $m = 0.5$, $c_1 = 17{,}000$ N/m$^{3/2}$. Figure 6 presents the fuel weight

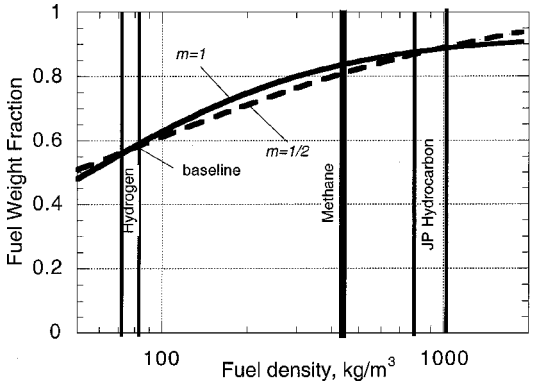

Fig. 6 Fuel weight fraction vs fuel density, modeled with constant thickness ($m = \frac{1}{2}$) and constant stress ($m = 1$) tanks.

fraction as a function of fuel density, for the limiting values of $m = 1$ and 0.5, based on the reference vehicle. For either value of m, if this same tank mass model were applicable to hydrocarbon, the equivalent-weight hydrocarbon cruise vehicle would have a fuel weight fraction greater than 0.8, which is certainly overly optimistic.

Lift-to-Drag Efficiency

As described earlier, one of the results of various optimized propulsion integration studies has been the realization that overall L/D with engine installation is generally lower than that promised by pure aerodynamic forms. For instance, the baseline configuration for the scaling studies shown in Fig. 4 is a fully integrated scramjet-powered craft optimized for maximum range performance with a scramjet engine. The airframe is derived from a hypersonic waverider inlet forebody, which is defined to provide high component L/D (Ref. 21). The engine-integrated vehicle has $L/D = 3.8$, compared to a pure waverider in this operating regime, which would be expected to have $L/D > 7$ (Refs. 19, 22–24). Clearly, the process of integrating the engine has reduced the delivered L/D performance.

This low value of realizable L/D can be attributed to the very low density of its hydrogen fuel; recall that overall density was 124 kg/m^3, including fuel, structure, and payload.[7,8] The optimizing code used to select the maximum range configuration matches lift to weight for level cruise flight, but altitude is fixed by the requirements of engine inlet conditions. This has the result that the shape that promises high L/D is operating at relatively low altitude, that is, high dynamic pressure, where it need only generate a fraction of the total available lift, and so actual L/D is smaller than the maximum achievable.

From this example, another way to view the effect of fuel selection on the vehicle performance is to calculate the actual L/D with Eq. (4), compared to the maximum attainable value defined in Eq. (2). Because fuel is consumed during flight, and lift requirements are therefore decreasing, L/D will also be changing throughout the flight. For most configurations of this type, flight L/D will be smaller than the maximum attainable L/D and will increase initially as weight is reduced, and so required lift is decreased. It is, thus, of interest to determine the best schedule for L/D. Note that, for conventional jet aircraft, it is well known that maximum range corresponds to a velocity that yields L/D that is 87% of the maximum L/D (Ref. 9). However, in the present work it is assumed that the vehicle flies at the maximum available velocity as dictated by propulsion and aerothermodynamics, without regard for identifying the velocity that delivers maximum range.

From the definition of Ω, we can write the L/D ratio at the beginning and the end of flight as

$$\left.\frac{L}{D}\right|_{\text{initial}} = \frac{2\Omega}{1+\Omega^2}\left[\frac{L}{D}\right]_{\max}$$

$$\left.\frac{L}{D}\right|_{\text{final}} = \frac{2[1-\varepsilon_c]\Omega}{1+[1-\varepsilon_c]^2\Omega^2}\left[\frac{L}{D}\right]_{\max} \tag{21}$$

from which it is clear that the initial L/D would be maximum if $\Omega = 1$ or that the final L/D would be maximum if $\Omega = 1/[1-\varepsilon]$. The value of Ω that provides maximum range for a given I_{sp} and flight velocity is found by solving for $dR/d\Omega = 0$ from Eq. (10):

$$\Omega_{\max_{\text{range}}} = \sqrt{1/(1-\varepsilon_c)} \tag{22}$$

The corresponding maximum achievable range is

$$R = \frac{2u_0 I_{sp}}{(1-\bar{g})}\left[\frac{L}{D}\right]_{\max} \tan^{-1}\left\{\frac{\varepsilon_c}{2\sqrt{1-\varepsilon_c}}\right\}$$

$$\cong \frac{u_0 I_{sp}}{(1-\bar{g})}\left[\frac{L}{D}\right]_{\max}\left\{\frac{\varepsilon_c\sqrt{1-\varepsilon_c}}{1-\varepsilon_c+0.07\varepsilon_c^2}\right\} \tag{23}$$

If the vehicle can be designed to satisfy this condition by appropriate selection of average density, then the maximum L/D during the flight approaches the aerodynamic limit. Interestingly, under these conditions, the initial and final values of L/D are equal:

$$\left.\frac{L}{D}\right|_{\text{initial}} = \left.\frac{L}{D}\right|_{\text{final}} = \frac{2\sqrt{1-\varepsilon_c}}{2-\varepsilon_c}\left[\frac{L}{D}\right]_{\max} \tag{24}$$

In other words, to achieve maximum range, the L/D starts out below the maximum, reaches a peak in the middle of the flight, and finishes with the same L/D with which it began. Maximizing L/D at either the beginning of cruise or end of cruise will not optimize overall performance. This optimal L/D schedule is equivalent to the results of Bowcutt, who performed detailed vehicle optimizations for maximum range.[25] Note that in the limit of a very high-density fuel, that is, $\varepsilon \to 1$, the maximum range value of Ω is infinity, and the initial and final values of L/D are zero. In the other limit of $\varepsilon \to 0$, in which the fuel has zero density, L/D is constant and equal to the maximum possible aerodynamic L/D, but the vehicle then has zero range.

This behavior is demonstrated in Fig. 7, which shows the actual L/D, divided by maximum achievable L/D, of a hypersonic vehicle at the beginning of cruise and the end of cruise, as a function of Ω. Note, for instance, that a vehicle that has $\Omega = 1$ begins with maximum L/D, but L/D that can drop by as little as 20% if the fuel weight fraction is 50%, or as much as 80% if the fuel weight fraction is 90%. Thus, an aircraft that is designed for $L/D = 6$, for example, will only have $L/D = 1.2$ at the end of its cruise. Similarly, a craft that is to have the maximum range at, for example, $\varepsilon = 0.7$, with a maximum achievable $L/D = 6$, will start with $L/D = 5.06$, peak at $L/D = 6$ somewhere in midflight, and then complete its cruise at $L/D = 5.06$ again.

The variation in L/D that is suggested by the results of Eq. (24) can be understood in the context of the L/D vs C_L plot of Fig. 1. Recall that, for given values of zero-lift drag and the constant of proportionality for drag due to lift k, there is a peak in L/D at a maximizing value of C_L. For optimum range performance, it is best

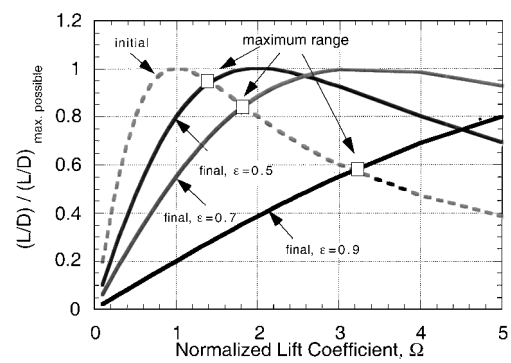

Fig. 7 Actual L/D, divided by maximum achievable aerodynamic L/D, as a function of normalized lift coefficient Ω: - - - -, is L/D at start of flight; ——, are L/D at end of flight for fuel weight fraction $\varepsilon = 0.5$, 0.7, and 0.9; also shown are the values of Ω which maximize range for each ε.

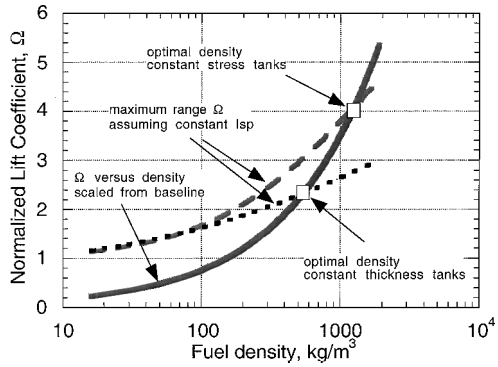

Fig. 8 Comparison of variation in normalized lift coefficient Ω and value of Ω that maximizes range for a fixed I_{sp}, under two assumptions for tank scaling, as a function of fuel density; intersection of these curves indicates density for maximum range performance.

to begin the flight at a C_L below the maximum and finish at a C_L above the maximum, so that the maximum is encountered along the way, with the vehicle crossing the L/D peak during its flight. Unfortunately, it will not always be possible to do this, given the available values of fuel density. Hydrogen vehicles tend to have performance in the region to the left of the L/D peak of Fig. 1. As demonstrated in this analysis, storable hydrocarbon vehicles hold the promise of operating closer to the peak.

Optimum Fuel Density

Given that there is an optimum value of Ω for each fuel weight ratio ε, and both Ω and ε depend on fuel density, there should be an optimal value of density that maximizes range. This is demonstrated graphically in Fig. 8, which plots the maximum range from Eq. (24) vs density, as well as the projected scaling of Ω with density from the baseline vehicle. Note that the optimum density is sensitive to tank weight scaling, but that in both cases shown, the best density is very close to that of storable hydrocarbon fuel.

These results are calculated assuming constant $u_0 I_{sp}$, which is equivlant to assuming constant overall efficiency. In fact, as pointed out earlier, the major advantage of the lower-density hydrogen fuels is their ability to deliver higher I_{sp}, possibly at higher efficiency than the hydrocarbon engine. If detailed data on I_{sp} vs fuel were available, it might be possible to incorporate I_{sp} variations in this analysis, which should decrease the optimal density for maximum range somewhat because lower density fuels tend to have higher I_{sp}. A combination of low-speed engines and high-speed engines, or proper scheduling for a combined-cycle engine, might be employed to optimize a cruiser's range.

Conclusions

The fundamental question explored in this effort is whether the packaging benefits of high-density hydrocarbon fuels outweigh the high-energy content of hydrogen fuels. For a cruiser operating in the Mach 8–10 corridor, in which it is desired to maximize cruise range for a given total takeoff weight, the result seems to be that the aerodynamic and volumetric advantages of storable hydrocarbons are about equivalent or superior to the I_{sp} advantages of hydrogen in determining cruiser range.

Of note is that methane seems to deliver the maximum range performance, because it combines high density with high specific energy content. It was found that a methane Mach 10 cruise vehicle in the 250,000-kg weight class would match the range of an equivalent weight hydrogen vehicle if its fuel weight fraction were greater than 0.65, compared to 0.55 for the hydrogen craft. A storable hydrocarbon vehicle with a fuel weight fraction of 0.72 would match the performance of a hydrogen craft. Both of these are appear to be reasonable goals, given the scaling of tank and structure weight with fuel volume. In fact, simple scaling laws predict fuel weight fractions of 0.76 and 0.82 for methane and storable hydrocarbon, respectively.

Given that methane is also a cryogenic liquid, the strong performance of the JP and endothermic hydrocarbon fuels suggests that they are the fuels of choice for a hypersonic cruiser. It is difficult to evaluate an intangible such as the penalty for handling a cryogen against a quantifiable range advantage, but it is likely that the 10% range improvement projected with methane is not worth the difficulties of using this fuel. At the very least, storable hydrocarbons can be refueled in flight, making for an enormous operational advantage.

Though not addressed directly here, centrifugal lift should tend to amplify the density effects demonstrated. At high velocity, centrifugal lift will decrease the effective density of a hypersonic craft, so that the benefits of higher density fuels would be even more evident. The role of engine lift might also be explored because that can have a large impact on overall L/D in the hypersonic regime.

The range results in this study depend greatly on the modeling of engine performance as a function of fuel. If a hydrocarbon scramjet can be built to operate more efficiently than a hydrogen-fueled engine, the performance benefits of the storable fuel would be even greater than suggested here. Conversely, if hydrogen engines prove more efficient, then the hydrocarbons will obviously be less favorable. Conclusions are also based on scaling from a baseline vehicle, and so only general trends should be drawn from this work. A more thorough validation of the fuel tradeoffs would require a more detailed vehicle design process, in which the best hydrogen cruiser is compared to the best hydrocarbon cruiser, including more detailed weight models, thermal protection, and I_{sp}. The success or failure of hydrocarbon-fueled scramjets, including the use of novel propulsion concepts, might obviously modify the derived results.

Acknowledgments

A portion of this effort was supported by NASA Grant NAGw-3175, with Isaiah M. Blankson as Technical Monitor, to whom appreciation is expressed. Blankson is also to be thanked for many insightful suggestions and technical comments that have been relevant to this work. Thanks also are extended to Ashwani Gupta of the Department of Mechanical Engineering at the University of Maryland, and especially Timothy Edwards of the U.S. Air Force Research Laboratory Propulsion Directorate for helpful suggestions and fuel data. Thanks are also expressed to Dilip R. Ballal of the University of Dayton for providing information on endothermic fuels.

References

[1] Kit, B., and Evered, D., *Rocket Propellant Handbook*, MacMillan, New York, 1960.

[2] "Survey of Jet Fuels (1990–1996)," Defense Energy Support Center, MIL-DTL-5624T, June 1998.

[3] Edwards, T., and Maurice, L. Q., "Surrogate Mixtures to Represent Complex Aviation and Rocket Fuels," AIAA Paper 99-2217, June 1999.

[4] Lefebvre, A., "Gas Turbine Fuels," *Gas Turbine Combustion*, Hemisphere, New York, 1983, Chap. 9.

[5] Sobel, D. R., and Spadaccini, L. J., "Hydrocarbon Fuel Cooling Technologies for Advanced Propulsion," *Journal of Engineering for Gas Turbines and Power*, Vol. 119, No. 2, 1997, pp. 344–351.

[6] Gurijanov, E., and Harsha, P., "New Directions in Hypersonic Technologies," AIAA Paper 96-4609, 1996.

[7] O'Neill, M. K., and Lewis, M. J., "Optimized Scramjet Integration on a Waverider," *Journal of Aircraft*, Vol. 29, No. 6, 1992, pp. 1114–1121.

[8] O'Neill, M. K., and Lewis, M. J., "Design Tradeoffs on Scramjet Engine Integrated Hypersonic Waverider Vehicles," *Journal of Aircraft*, Vol. 30, No. 6, 1993, pp. 943–952.

[9] Raymer, D. P., *Aircraft Design: A Conceptual Approach*, 3rd ed., edited by J. S. Przemieniecki, AIAA Education Series, AIAA, Reston, VA, 1999, pp. 16–18.

[10] Speyer, J., "Periodic Optimal Flight," *Journal of Aircraft*, Vol. 19, No. 4, 1996, pp. 745–755.

[11] Bryson, A. E., Desai, M. N., and Hoffman, W. C., "Energy State Approximation in Performance Optimization of Supersonic Aircraft," *Journal of Aircraft*, Vol. 6, No. 6, 1969, pp. 481–488.

[12] Rasmussen, M., *Hypersonic Flow*, Wiley, New York, 1994, p. 67.

[13] Gillum, M., and Lewis, M. J., "Analysis of Experimental Results on a Mach 14 Waverider with Blunt Leading Edges," *Journal of Aircraft*, Vol. 34, No. 3, 1997, pp. 296–303.

[14] Bert, C., "Prediction of Range and Endurance of Jet Aircraft at Constant

Altitude," *Journal of Aircraft*, Vol. 18, No. 10, 1981, pp. 890–892.

[15]Kerrebrock, J. L., *Aircraft Engines and Gas Turbines*, 2nd ed., MIT Press, Cambridge, MA, 1995, pp. 5, 6.

[16]Kerrebrock, J. L., "Some Readily Quantifiable Aspects of Scramjet Engine Performance," *Journal of Propulsion and Power*, Vol. 8, No. 5, 1992, pp. 1116–1122.

[17]Takashima, N., and Lewis, M. J., "Optimization of Waverider-Based Cruise Vehicles with Off-Design Considerations," *Journal of Aircraft*, Vol. 36, No. 1, 1999, pp. 235–245.

[18]Takashima, N., and Lewis, M. J., Lockwood, M. K., and Bogar, T., "Waverider Configuration Development for the Dual Fuel Vehicle" AIAA Paper 96-4593, Nov. 1996.

[19]Starkey, R., and Lewis, M. J., "Simple Analytical Model for Parametric Studies of Hypersonic Waveriders," *Journal of Spacecraft and Rockets*, Vol. 36, No. 4, 1999, pp. 516–523.

[20]Glatt, C. R., "Watts—A Computer Program for Weights Anaylsis of Advanced Transportation Systems," NASA CR-2420, Sept. 1974.

[21]Nonweiler, T. R. F., "Aerodynamic Problems of Manned Space Vehicles," *Journal of the Royal Aeronautical Society*, Vol. 63, No. 585, 1959, pp. 521–528.

[22]Takashima, N., and Lewis, M. J., "A Cone-Wedge Waverider Configuration for Engine–Airframe Integration," *Journal of Aircraft*, Vol. 32, No. 5, 1995, pp. 1142–144.

[23]Takashima, N., and Lewis, M., "Waverider Configurations Based on Nonaxisymmetric Flow Fields for Engine–Airframe Integration," AIAA Paper 94-0380, Jan. 1994.

[24]Takashima, N., and Lewis, M. J., "Navier–Stokes Computations of Hypersonic Viscous Optimized Waveriders," *Journal of Spacecraft and Rockets*, Vol. 31, No. 3, 1994, pp. 383–391.

[25]Bowcutt, K. G., "Multidisciplinary Optimization of Airbreathing Hypersonic Vehicles," *Journal of Propulsion and Power*, Vol. 17, No. 6, 2001, pp. 1184–1190.